4518 *Inorg. Chem.* **2010**, *49*, 4518–4523
DOI: 10.1021/ic902462k

Inorganic Chemistry
Article

A Functional Model of Extradiol-Cleaving Catechol Dioxygenases: Mimicking the 2-His-1-Carboxylate Facial Triad

Sayantan Paria, Partha Halder, and Tapan Kanti Paine*

Department of Inorganic Chemistry, Indian Association for the Cultivation of Science (IACS), 2A and 2B Raja S. C. Mullick Road, Jadavpur, Kolkata 700032, India

Received December 11, 2009

The synthesis and characterization of an iron−catecholate model complex of a tridentate 2-*N*-1-carboxylate ligand derived from L-proline are reported. The X-ray crystal structure of the complex $[(L)_3Fe_3(DBC)_3]$ (**1**) (where L is 1-(2-pyridylmethyl)pyrrolidine-2-carboxylate and DBC is the dianion of 3,5-di-*tert*-butyl catechol) reveals that the tridentate ligand binds to the iron center in a facial manner and mimics the 2-his-1-carboxylate facial triad motif observed in extradiol-cleaving catechol dioxygenases. The iron(III)−catecholate complex (**1**) reacts with dioxygen in acetonitrile in ambient conditions to cleave the C−C bond of catecholate. In the reaction, an equal amount of extra- and intradiol cleavage products are formed without any auto-oxidation product. The iron−catecholate complex is a potential functional model of extradiol-cleaving catechol dioxygenases.

Introduction

Catechol dioxygenases are nonheme iron enzymes that catalyze the C−C bond cleavage of aromatic *cis*-diols by the use of aerial oxygen as the oxidant.[1,2] Catechol dioxygenases are classified, depending on the position of the C−C bond cleavage, into two categories.[1] In the active site of intradiol dioxygenases, iron(III) is ligated by two histidines and two tyrosinates in the resting state.[3] The extradiol-cleaving dioxygenases use an octahedral iron(II) center coordinated by two histidines and one carboxylate ligand in one face, leaving the other face for exogenous ligands.[1,4]

The 2-his-1-carboxylate facial triad[5−7] is a common structural motif in the super family of nonheme iron enzymes. Many efforts were made to mimic the structural and functional aspects of this enzymes family over the last decades.[1] A large number of iron−catecholate model complexes are reported where tetradentate N_4,[8−12] N_3O,[13,14] or tridentate N_2O[15,16] donor ligands are employed. The model complexes show a diverse C−C bond cleavage reactivity. A limited number of iron−catecholate complexes of facial tridentate N_3 ligands, like 1,4,7-triazacyclononane (TACN),[17,18] Me_3−TACN,[19] and Tp^{iPr2} [20] are reported that selectively give extradiol cleavage products. Among the reported models, the iron complex of TACN has been shown to exhibit high selectivity, and around 98% extradiol cleavage products were obtained.[17] Iron−catecholate model complexes that mimic the 2-*N*-1-carboxylate facial coordination motif, as observed in the active site of extradiol-cleaving catechol dioxygenases, are rare. Gebbink et al.[21] have recently reported iron−catecholate complexes, where the iron is coordinated by

*Corresponding author. Phone: +91-33-2473-4971. Fax: +91-33-2473-2805. E-mail: ictkp@iacs.res.in.

(1) Costas, M.; Mehn, M. P.; Jensen, M. P.; Que, L., Jr. *Chem. Rev.* **2004**, *104*, 939–986.
(2) Bugg, T. D. H.; Lin, G. *Chem. Commun.* **2001**, *11*, 941–952.
(3) Ohlendorf, D. H.; Lipscomb, J. D.; Weber, P. C. *Nature* **1988**, *336*, 403–405.
(4) Kovaleva, E. G.; Lipscomb, J. D. *Science* **2007**, *316*, 453–457.
(5) Hegg, E. L.; Que, L., Jr. *Eur. J. Biochem.* **1997**, *250*, 625–629.
(6) Que, L., Jr. *Nat. Struct. Biol.* **2000**, *7*, 182–184.
(7) Straganz, G. D.; Nidetzky, B. *ChemBioChem* **2006**, *7*, 1536–1548.
(8) Jang, H. G.; Cox, D. D.; Que, L., Jr. *J. Am. Chem. Soc.* **1991**, *113*, 9200–9204.
(9) Koch, W. O.; Krüger, H.-J. *Angew. Chem., Int. Ed. Engl.* **1995**, *34*, 2671–2674.
(10) Jo, D.-H.; Chiou, Y.-M.; Que, L., Jr. *Inorg. Chem.* **2001**, *40*, 3181–3190.
(11) Raffard, N.; Carina, R.; Simaan, A. J.; Sainton, J.; Rivière, E.; Tchertanov, L.; Bourcier, S.; Bouchoux, G.; Delroisse, M.; Banse, F.; Girerd, J.-J. *Eur. J. Inorg. Chem.* **2001**, 2249–2254.
(12) Mayilmurugan, R.; Stoeckli-Evans, H.; Palaniandavar, M. *Inorg. Chem.* **2008**, *47*, 6645–6658.
(13) Cox, D. D.; Que, L., Jr. *J. Am. Chem. Soc.* **1988**, *110*, 8085–8092.
(14) Li, F.; Wang, M.; Li, P.; Zhang, T.; Sun, L. *Inorg. Chem.* **2007**, *46*, 9364–9371.
(15) Panda, M. K.; John, A.; Shaikh, M. M.; Ghosh, P. *Inorg. Chem.* **2008**, *47*, 11847–11856.
(16) Bruijnincx, P. C. A.; Lutz, M.; Spek, A. L.; Hagen, W. R.; van Koten, G.; Gebbink, R. J. M. K. *Inorg. Chem.* **2007**, *46*, 8391–8402.
(17) Ito, M.; Que, L., Jr. *Angew. Chem., Int. Ed. Engl.* **1997**, *36*, 1342–1344.
(18) Lin, G.; Reid, G.; Bugg, T. D. H. *J. Am. Chem. Soc.* **2001**, *123*, 5030–5039.
(19) Jo, D.-H.; Que, L., Jr. *Angew. Chem., Int. Ed. Engl.* **2000**, *39*, 4284–4287.
(20) Ogihara, T.; Hikichi, S.; Akita, M.; Moro-oka, Y. *Inorg. Chem.* **1998**, *37*, 2614–2615.
(21) Bruijnincx, P. C. A.; Lutz, M.; Spek, A. L.; Hagen, W. R.; Weckhuysen, B. M.; van Koten, G.; Gebbink, R. J. M. K. *J. Am. Chem. Soc.* **2007**, *129*, 2275–2286.

 Published on Web 04/14/2010

Chart 1. Ligands

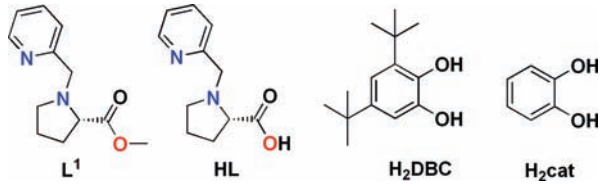

facial *N,N,O* donor ligands, closely mimicking the active site of extradiol-cleaving catechol dioxygenases. The model complexes react with dioxygen to give mainly the auto-oxidation product of catechol along with a maximum of 38% extradiol cleavage products. This work stems from our interest in designing structural and functional models of nonheme iron enzymes with the 2-his-1-carboxylate facial triad. In this paper, we report the syntheses and characterization of iron−catecholate complexes, $[(L)_3Fe_3(DBC)_3]$ (**1**) and $[(L)_3Fe_3(cat)_3]$ (**2**), of a proline-based flexible tridentate facial ligand (HL = 1-(2-pyridylmethyl)pyrrolidine-2-carboxylic acid) containing two nitrogen and one carboxylate oxygen donors (Chart 1). The molecular structure of **1** was obtained by the single crystal X-ray diffraction studies. We also report herein the reactivity of iron−catecholate complexes toward dioxygen and the selectivity of the C−C bond cleavage of catechol.

Experimental Section

General. All chemicals and solvents were purchased from commercial sources and were used without further purification unless otherwise noted. Solvents were distilled, dried, and deoxygenated before use. 2-Methoxycarbonyl-1-(2-pyridylmethyl)pyrrolidine (L^1) was prepared by a modification of the literature procedure.[22] Caution: Although no problems were encountered during the synthesis of the complex, perchlorate salts are potentially explosive and should be handled with care![23] Preparation and handling of air-sensitive materials were carried out under an inert atmosphere either in a glovebox or in a Schlenk line.

Synthesis of HL. The ester L^1 (0.11 g, 0.5 mmol) was dissolved in 1 mL of 1 M sodium hydroxide solution at 0 °C on an ice bath. The ice bath was then removed, and the mixture was allowed to stir for 6 h at room temperature (RT). The solution was maintained at pH = 7, and aqueous layer was extracted with dichloromethane. The aqueous phase was removed under vacuum to give a yellow residue. The residue was treated with absolute alcohol, and sodium chloride was separated by filtration. Removal of ethanol gave the pure ligand HL as light-yellow oil. Yield: 0.08 g (78%). ESI-MS (positive ion mode, CH_3CN): m/z = 229.00 (100%, [(HL) + Na]$^+$), 207.03 (25%, [(HL) + H]$^+$), 161.04 (10%, [(HL) − COOH]$^+$). ^{1}H NMR (300 MHz, CD_2Cl_2): δ = 8.51 (d, 1H, J = 4.2 Hz), 7.64 (m, 1H), 7.37 (d, 1H, J = 7.7 Hz), 7.20 (m, 1H), 4.26 (d, 1H, J = 14.2 Hz), 4.21 (d, 1H, J = 14.1 Hz), 3.92 (m, 1H), 3.50 (m, 1H), 2.92 (m, 1H), 2.23 (m, 2H), 1.89 ppm (m, 2H).

$[(L)_3Fe_3(DBC)_3]$ (1). Ligand HL (0.103 g, 0.5 mmol) was dissolved in methanol (5 mL). To that, a methanolic solution (5 mL) of iron(III) perchlorate hydrate (0.18 g, 0.5 mmol) was added with stirring. The color of the solution changed to reddish brown. A mixture of 3,5-di-*tert*-butyl catechol (0.11 g, 0.5 mmol), and triethylamine (140 μL, 1 mmol) in methanol (2 mL) was added to the reaction mixture. The color of the mixture immediately took deep purple-blue. The mixture was allowed to stir for 2 h and solvent was removed under vacuum to give a deep purple-blue solid. This crude solid was then washed several times with deionized water to remove the salts, and finally dried under vacuum to give a pure compound. Yield: 0.22 g (92%). X-ray quality single crystals of $\mathbf{1}\cdot NaBPh_4$ were grown by slow diffusion of hexane into an acetonitrile solution of **1** in the presence of sodium tetraphenylborate. Elemental analysis calcd (%) for $C_{75}H_{99}Fe_3N_6O_{12}$ (1444.16 g/mol): C 62.38, H 6.91, N 5.82; Found: C 61.9, H 6.7, N 5.8. IR (KBr): υ = 3430(br), 2954(vs), 1737(w), 1636−1612(br), 1470(s), 1446(s), 1414(s), 1360(s), 1247(s), 1114(s), 982(m), 761(s), 727(m), 678(s) cm^{-1}. ESI-MS (positive ion mode, CH_3CN): m/z = 1465.10 (10%, [{$L_3Fe_3(DBC)_3$} + Na]$^+$), 984.95 (50%, [{$L_2Fe_2(DBC)_2$} + Na]$^+$), 962.98 (10%, [{$L_2Fe_2(DBC)_2$} + H]$^+$), 504.01 (100%, [{LFe(DBC)} + Na]$^+$), 482.03 (60%, [{LFe(DBC)} + H]$^+$), 243.05 (70%, [DBC + Na]$^+$), 221.06 (25%, [DBC + H]$^+$). UV−vis (in MeCN): λ, nm (ε, M^{-1}cm^{-1}): 715 (4100), 500 (3450), 325 (sh).

$[(L)_3Fe_3(cat)_3]$ (2). To a warm mixture of HL (0.206 g, 1 mmol), sodium hydroxide (0.04 g, 1 mmol), and iron(III) perchlorate (0.354 g, 1 mmol) in 5 mL of methanol was dopwise added a methanolic solution (5 mL) of a mixture of catechol (0.10 g, 1 mmol) and sodium hydroxide (0.08 g, 2 mmol). The color of the solution immediately turned to purple-blue. The mixture was then stirred under warm conditions for 1 h. The solution was concentrated under vacuum, and then diethylether (5 mL) was added to the mixture. A blue precipitate was separated upon cooling, which was isolated by filtation and dried under vacuum. Yield: 0.28 g (68%). Elemental analysis calcd (%) for $C_{51}H_{51}Fe_3N_6O_{12}\cdot NaClO_4$(1229.96 g/mol): C 49.80, H 4.18, N 6.83; Found: C 49.3, H 4.3, N 6.4. IR (KBr): υ = 3423(br), 2926(vs), 1640−1616(br), 1462(s), 1390(s), 1252(s), 1095(vs), 1028(s), 870(m), 787(s), 741(s), 671(s), 648(s), 623(s) cm^{-1}. ESI-MS (positive ion mode, CH_3CN): m/z (%): 1128.84 (15%, [{$L_3Fe_3(cat)_3$} + Na]$^+$), 760.32 (50%, [{$L_2Fe_2(cat)_2$} + Na]$^+$), 652.41 (25%, [{$L_2Fe_2(cat)$} + Na]$^+$), 391.64 (100%, [{LFe(cat)} + Na]$^+$), 369.69 (10%, [{LFe(cat)} + H]$^+$). UV−vis (in MeCN): λ, nm (ε, M^{-1}cm^{-1}): 600 (3050), 400 (2900), 330 (sh).

Analyses of 3,5-Di-*tert*-butyl Catechol Cleavage Products. 60 mg (0.04 mmol) of complex **1** was dissolved in an organic solvent (15 mL). Dioxygen was bubbled through the solution for two minutes and then allowed to stir for 12 h at RT under oxygen atmosphere. The purple-blue solution slowly turned to green. To the solution, one equivalent of internal standard (1,3,5-tribromobenzene) was added, and the solvent was removed under reduced pressure. The residue was then treated with 10 mL of 3 M HCl, the organic products were extracted with diethylether (3 × 15 mL) and dried over sodium sulfate. Removal of solvent gave the catechol cleavage products. The organic products were analyzed by ESI-MS without further purification and were quantified by ^{1}H NMR spectroscopy. Authentic compounds were prepared according to the literature procedure or compared the spectral data with the reported compounds.[24−27] RT ^{1}H NMR data for 3,5-di-*tert*-butyl catechol cleavage products (300 MHz, $CDCl_3$): δ = 4,6-di-*tert*-butyl-2-pyrone (**A**): 1.22 (s, 9H), 1.36 (s, 9H), 6.05 (m, 2H); 3,5-di-*tert*-butyl-2-pyrone (**B**): δ = 1.22 (s, 9H), 1.40 (s, 9H), 7.21 (d, 1H), 7.24 (d, 1H); *cis,cis*-3,5-di-*tert*-butyl-2-hydroxymuconic semialdehyde (**C**): δ = 1.11 (s, 9H), 1.19 (s, 1H), 5.90 (s, 1H), 9.60 (s, 1H); 3,5-di-*tert*-butyl-1-oxacyclohepta-3,5-diene-2,7-dione (**D**): δ = 1.16 (s, 9H), 1.28 (s, 1H), 6.14 (d, 1H), 6.44 (d, 1H); 3,5-di-*tert*-butyl-5-(carboxymethyl)-2-furanone (**E**): δ = 0.98 (s, 9H), 1.24 (s, 9H), 2.91 (d, 1H), 2.81 (d, 1H), 6.96 (s, 1H), 9.72 (s, 1H); 3-*tert*-butylfuran-2,5-dione (**F**): 1.33(s, 9H),

(22) Chelucci, G.; Falorni, M.; Giacomelli, G. *Tetrahedron: Asymmetry* **1990**, *1*, 843–849.
(23) Wolsey, W. C. *J. Chem. Educ.* **1973**, *50*, A335–A337.
(24) Demmin, T. R.; Rogic, M. M. *J. Org. Chem.* **1980**, *45*, 1153–1156.
(25) Matsumoto, M.; Kuroda, K. *J. Am. Chem. Soc.* **1982**, *104*, 1433–1434.
(26) Weiner, H.; Hayashi, Y.; Finke, R. G. *Inorg. Chim. Acta* **1999**, *291*, 426–437.
(27) Mayilmurugan, R.; Suresh, E.; Palaniandavar, M. *Inorg. Chem.* **2007**, *46*, 6038–6049.

Table 1. Crystallographic Data for Complex $1 \cdot NaBPh_4$

	$1 \cdot NaBPh_4$
empirical formula	$C_{99}H_{119}BFe_3N_6NaO_{12}$
formula weight	1786.35
crystal system	trigonal
space group	*R*3
a, Å	17.4081(4)
b, Å	17.4081(4)
c, Å	27.0084(14)
α, °	90.00°
β, °	90.00°
γ, °	120.00°
volume, Å^3	7088.1(4)
Z	3
$D_{calcd.}$, Mg/m^3	1.255
μ Mo Kα, mm^{-1}	0.521
F(000)	2835
θ range, °	1.55−31.81
reflections collected	29 657
reflns unique	8930
R(int)	0.0238
data ($I > 2\sigma(I)$)	7576
parameters refined	343
goodness-of-fit on F^2	1.048
R1 [$I > 2\sigma(I)$]	0.0637
*wR*2	0.1748
residuals e.Å^{-3}	0.733−2.875

6.52(s, 1H); and 3,5-di-*tert*-butylbenzoquinone (**Q**): δ = 1.22 (s, 9H), 1.28 (s, 9H), 6.21 (d, 1H), 6.93 (d, 1H).

Physical Measurements. Fourier transform infrared spectroscopy on KBr pellets was performed on a Shimadzu FT-IR 8400S instrument. Elemental analyses were performed on a Perkin-Elmer 2400 series II CHN series. Solution electronic spectra were measured on an Agilent 8453 diode array spectrophotometer. Electro-spray mass spectra were recorded with a Waters QTOF Micro YA263 instrument. All RT ^{1}H NMR spectra were collected on a Bruker DPX-300 spectrometer.

X-ray Crystal Structure Determination. Crystallographic data for **1** are provided in Table 1. X-ray single crystal data for $1 \cdot NaBPh_4$ were collected at 100 K using Mo Kα (λ = 0.7107 Å) radiation on a SMART APEX diffractometer equipped with CCD area detector. Data collection and reduction and structure solution/refinement were carried out using the software package of APEX II.[28] All structures were solved by direct method and refined in a routine manner. The non-hydrogen atoms were treated anisotropically. The disordered carbons were treated isotropically. The hydrogen atoms were geometrically fixed, except those that are attached with disordered carbon atoms. The tetraphenyl borate counteranion is found to be disordered on a three-fold axis. The isotropic thermal parameters of disorder carbon atoms of the phenyl ring which lie on three-fold axis were fixed, and the other three phenyl rings and one tertiary butyl group were refined isotropically using the second free variable facility (FVAR) provided with SHELXTL,[29] so the total site occupancy factor (SOFs) of the disordered atom is 1.

Results and Discussion

The ligand (HL) was synthesized, according to a modification of the reported procedure,[22] by reductive amination of pridine-2-carboxaldehyde with L-proline methyl ester hydrochloride using sodium cyanoborohydride in methanol followed by hydrolysis of the ester (Scheme 1). The iron(III)−catecholate complexes were synthesized by reacting the ligand, iron(III) perchlorate, catechol, and base (1:1:1:3) in methanol (Scheme 1). Complex **1** can also be synthesized by reacting L^1 with an iron(III) salt and 3,5-di-*tert*-butyl catechol in the presence of a base. The ester gets hydrolyzed during the reaction with concomitant formation of the catecholate complex. Electro-spray ionization mass spectrometry (ESI-MS) of **1** in acetonitrile shows predominant peaks at *m*/*z* 1465.10, 984.95, 504.00, and 482.03, with isotope distribution patterns calculated for $[\{(L)_3Fe_3(DBC)_3 + Na\}]^+$, $[\{(L)_2Fe_2(DBC)_2\} + Na]^+$, $[\{(L)Fe(DBC)\} + Na]^+$ and $[\{(L)Fe(DBC)\} + H]^+$, respectively. ESI-MS (positive ion mode) of **2** in acetonitrile shows peaks at *m*/*z* 1128.84, 760.32, 652.41, 391.64, and 369.69, with expected isotope distribution patterns calculated for $[\{L_3Fe_3(cat)_3\} + Na]^+$, $[\{L_2Fe_2(cat)_2\} + Na]^+$, $[\{L_2Fe_2(cat)\} + Na]^+$, $[\{LFe(cat)\} + Na]^+$, and $[\{LFe(cat)\} + H]^+$ ions, respectively. This indicates that trinuclear species dissociate in solution. It is also possible that the trinuclear species get decomposed in the experimental condition of mass spectrometry. Interestingly, the ESI-MS of an acetonitrile solution containing both **1** and **2** shows additional peaks at *m*/*z* 1395.99, 1354.19, 1134.37, and 873.40, attributable to $[\{L_3Fe_3(DBC)_2(cat)(MeCN)\} + Na]^+$, $[\{L_3Fe_3(DBC)_2(cat)\} + Na]^+$, $[\{L_3Fe_3(DBC)(cat)\} + Na]^+$, and $[\{L_2Fe_2(DBC)(cat)\} + Na]^+$, respectively. The detection of peaks corresponding to mixed catecholate species establishes the existence of an equilibrium among mono-, di- and trinuclear species in solution. The deep-blue complex **1** shows two strong bands at 715 and 500 nm in acetonitrile typical for catecholate-to-iron(III) charge-transfer transitions.[13] The charge-transfer bands for complex **2**, on the other hand, are shifted to higher energy at 600 and 400 nm. The shifting of the charge-transfer band to higher energy for **2** with respect to **1** is due to the absence of electron-donating substituent on the catecholate ring in **2**.[30]

Scheme 1. Synthesis of Ligand and Iron−Catecholate Complexes

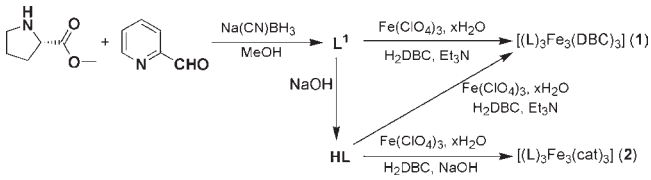

Crystal Structure. X-ray quality single crystals of $1 \cdot NaBPh_4$, crystallized in a chiral space group trigonal *R*3, were grown by slow diffusion of hexane into an acetonitrile solution in the presence of sodium tetraphenyl borate. It is important to note that the complex could not be crystallized in the absence of sodium salt. The role of sodium ion in the crystallization process can be explained from the structure of **1** (Figure 1), which exhibits a cyclic trinuclear complex with three 3,5-di-*tert*-butyl catecholates, three irons, and three ligands forming a sodium ion encapsulated 12-MC-3 metallacoronate.[31] In the monocationic C3 symmetric trinuclear complex, each iron center is in octahedral environment coordinated by the tridentate *N*,*N*,*O* ligand occupying one face of the octahedron and a bidentate catecholate. The remaining sixth coordination site is occupied by a bridging carboxylate oxygen atom from another ligand.

(28) *Bruker*, version 2.1−0; Bruker AXS, Inc.: Madison, WI, **2006**.
(29) Sheldrick, G. M. *SHELXL-97, Program for crystal structure refinement*; University of Göttingen: Göttingen, Germany, 1997.
(30) Cox, D. D.; Benkovic, S. J.; Bloom, L. M.; Bradley, F. C.; Nelson, M. J.; Que, L., Jr.; Wallick, D. E. *J. Am. Chem. Soc.* **1988**, *110*, 2026–2032.
(31) Mezei, G.; Zaleski, C. M.; Pecoraro, V. L. *Chem. Rev.* **2007**, *107*, 4933–5003.

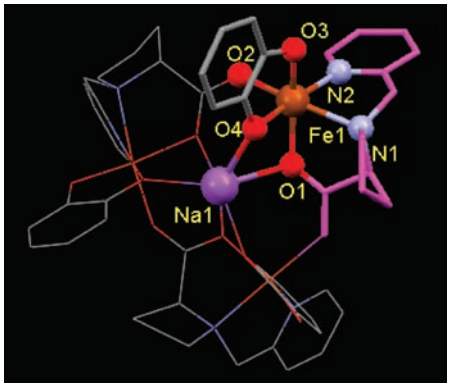

Figure 1. Crystal structure of sodium encapsulated $[(L)_3Fe_3(DBC)_3]$. The hydrogen atoms and *tert*-butyl groups (on catechols) are omitted for clarity.

Table 2. Selected Bond Lengths (Å) and Angles (°) for **1**·$NaBPh_4$

Fe(1)−N(1)	2.228(3)	C(12)−C(25)	1.403(4)
Fe(1)−N(2)	2.145(3)	C(12)−C(13)	1.414(5)
Fe(1)−O(1)	2.039(2)	C(13)−C(18)	1.385(6)
Fe(1)−O(3)	1.908(2)	C(18)−C(19)	1.395(6)
Fe(1)−O(4)	1.951(2)	C(19)−C(24)	1.391(5)
Fe(1)−O(2)	2.068(3)	C(24)−C(25)	1.386(4)
Na(1)−O(1)	2.443(3)	O(3)−C(12)	1.344(4)
Na(1)−O(4)	2.250(2)	O(4)−C(25)	1.350(4)
O(2)−Fe(1)−N(1)	162.26(11)	O(4)−Fe(1)−N(2)	176.01(13)
O(1)−Fe(1)−O(3)	163.95(11)	O(3)−Fe(1)−O(4)	83.43(10)
O(1)−Fe(1)−N(2)	96.18(11)	O(3)−Fe(1)−O(2)	94.41(11)
O(1)−Fe(1)−O(2)	96.18(11)	N(2)−Fe(1)−N(1)	76.58(12)
O(4)−Fe(1)−O(1)	83.43(10)	O(2)−Fe(1)−N(2)	87.61(12)
O(4)−Fe(1)−N(1)	99.47(11)	O(4)−Fe(1)−O(2)	96.38(10)
O(3)−Fe(1)−N(2)	96.28(12)	O(3)−Fe(1)−N(1)	95.25(11)

In each of the [(L)Fe(DBC)] unit of **1**, one catecholate oxygen atom (O4) and the pyridine nitrogen atom (N2) occupy the axial position and are *trans* to each other (O4−Fe1−N2 angle at 176.01(13)°) with the Fe1−O4 and Fe1−N2 distances of 1.951(2) and 2.145(3) Å, respectively. The other catecholate oxygen atom (O3) occupies a position in the equatorial plane *trans* to the carboxylate oxygen atom (O1) from the ligand with the Fe1−O3 and Fe1−O1 distances of 1.908(2) and 2.039(2) Å, respectively. The C−O and C−C bond lengths of the catecholate ring indicate the binding of dianionic catecholate (Table 2). It is important to note that the catecholate oxygens bind to the iron center *trans* to the histidine nitrogen atoms leaving the site *trans* to carboxylate donor for the activation of dioxygen, as observed in the structure of extradiol dioxygenase.[4] In complex **1**, two other positions in the equatorial plane are occupied by the amine nitrogen N1 (Fe1−N1 at 2.228(3) Å) and a bridging carboxylate oxygen atom O2 (Fe1−O2 at 2.068(3) Å) from another ligand with the O2−Fe1−N1 angle of 162.26(11)°. The Fe−N and Fe−O (catecholate) bond distances are closely comparable to the reported [(TPA)-Fe(DBC)]BPh_4 complex,[8] while the Fe−O(carboxylate) distances are slightly longer than those reported in related complexes.[13,21] The encapsulated sodium ion is in an octahedral coordination environment ligated by catecholate oxygen (O4) and carboxylate oxygen (O1) atoms.

Reactivity of Catecholate Complexes toward Dioxygen. The reactivity of **1** toward dioxygen was investigated to determine the catechol cleavage products. The deep blue solution of **1** reacts with dioxygen in acetonitrile at ambient conditions over a period of 2 h to give a green solution. During the reaction, the catecholate-to-iron(III) charge-transfer bands at 715 and 500 nm slowly disappear with time at a rate of 5.15×10^{-4} s^{-1}. The disappearance of the charge-transfer bands (Figure 2) indicates the oxidation of bound catecholate. The rate of the reaction becomes slighter slower in dichloromethane ($k_{obs} = 3.31 \times 10^{-4}$ s^{-1}).

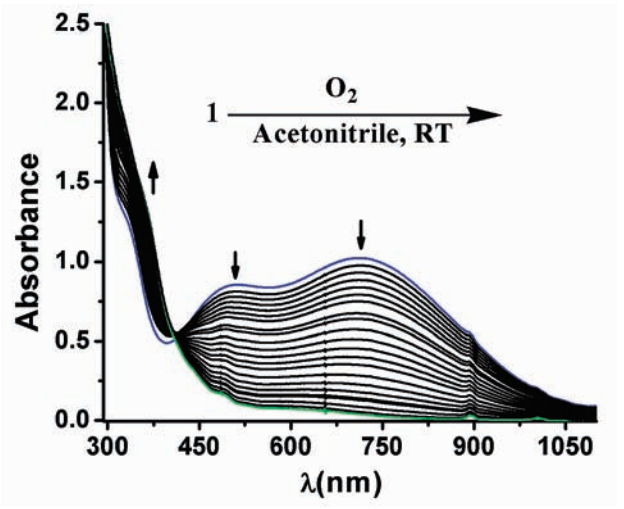

Figure 2. UV−vis spectral changes of complex **1** (conc. = 0.25 mM) in MeCN upon exposure to dioxygen at ambient condition.

Further, the oxidized products from 3,5-di-*tert*-butyl catechol were identified by ^{1}H NMR spectroscopy and by comparing with independently synthesized compounds or their known spectra. The products were quantified by ^{1}H NMR spectroscopy using 1,3,5-tribromobenzene as an internal standard. The distribution of catechol-derived products was found to be solvent dependent. In the reaction of **1** with O_2 in acetonitrile, 42% of extradiol cleavage products were obtained along with the formation of same percentage of intradiol cleavage products (Table 3). In this reaction, a small amount (4%) of a five-membered ring, 3-*tert*-butylfuran-2,5-dione (**F**), was formed as a side product. The amount of organic product from catechol cleavage accounts for 88% of 3,5-di-*tert*-butyl catechol. The remaining 12% was accounted as unreacted substrate. The percentage of auto-oxidation product, 3,5-di-*tert*-butylbenzoquinone, was found to be negligible. In contrast, in the work of Gebbink et al.[21] with a model iron−catecholate complex of a facial *N*,*N*,*O* donor ligand, the major product was the quinone. Therefore, the model complex reported here is an improvement over the reported catecholate complexes supported by *N*,*N*,*O* donor ligands. The product distribution changed dramatically in dichloromethane with a decrease in extra- and intradiol cleavage products. In this case, about 13% auto-oxidation product of catechol was observed.

While complex **1** reacts with oxygen to form 3,5-di-*tert*-butyl catechol cleavage products, complex **2** is unreactive toward O_2 under similar conditions and does not give any catechol cleavage product. This may be due the fact that the unsubstituted catecholate ring is not sufficiently electron rich to form iron(II)−semiquinone species for further reaction with dioxygen.

To understand the role of metal valency on the selectivity of C−C bond cleavage, the reactivity of iron(II)−catecholate complex toward dioxygen was studied.

Table 3. Catechol Cleavage Products upon Reaction of **1** with O_2

Complex	solvent	% extradiol (A+B+C)	% intradiol (D+E)	% others (F+Q)	% conversion
1	MeCN	42(32+10+0)	42(26+16)	4 (4+0)	88
1	CH_2Cl_2	26(22+4+0)	25(12+13)	21(8+13)	72
Fe(II)+HL+ H_2DBC+TEA	MeCN	36(21+6+9)	34(22+12)	3 (3+0)	73

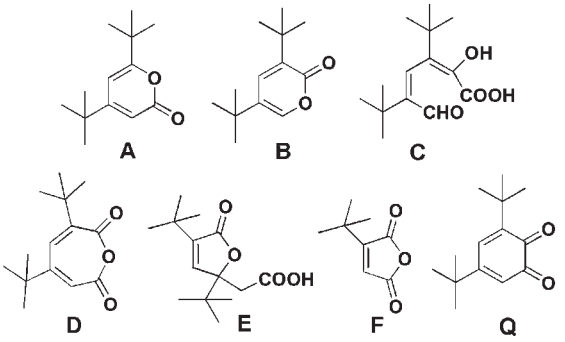

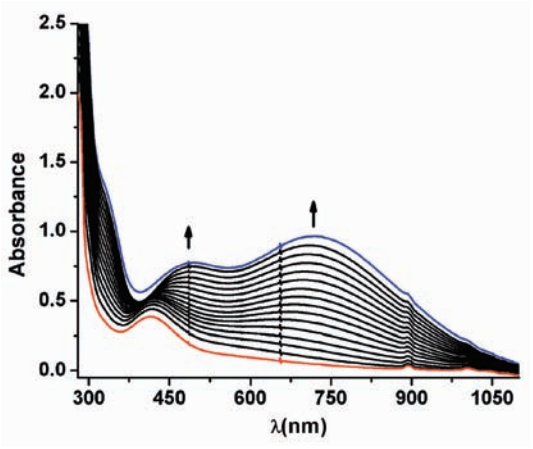

Figure 3. UV−vis spectral changes of iron(II)−catecholate complex prepared in situ (conc. = 0.75 mM of $Fe(ClO_4)\cdot 6H_2O$, HL, and H_2DBC and 1.5 mM of Et_3N) in MeCN upon exposure to dioxygen at 50 °C.

Several attempts to isolate an iron(II)−catechloate complex of HL were failed. The iron(II)−catecholate complex of HL was prepared in situ at 50 °C in acetonitrile. Initially a yellow solution was formed which slowly changed to purple-blue in the presence of dioxygen (Figure 3). The optical spectrum of the purple-blue species was found to be exactly similar to that of the iron(III)−catecholate complex **1**. The purple-blue iron(III)−catecholate species further changed to a green solution as observed for **1**. This supports the proposal by Que et al.[10] and Moro-oka et al.[20] that the iron(II)−catecholate complex is oxidized to iron(III)−catecholate complex by an outer-sphere electron transfer followed by the attack of O_2 to form an iron(III)−peroxide intermediate. In this case, the isolated products from the reaction mixture showed similar distribution of products with about 36% extradiol, 34% intradiol cleavage, and no auto-oxidation product (Table 3). It is worth mentioning here about the formation of 9% of an extradiol cleavage product, *cis*,*cis*-3,5-di-*tert*-butyl-2-hydroxy muconic semialdehyde (**C**), which is rarely reported in model studies.[26,27] This product is formed as a result of hydrolysis of the lactone ring in the extradiol cleavage pathway. However, product **C** was observed only during the reaction with in situ generated complexes but not with **1**. The use of iron(II) did not change the selectivity of extradiol products.

The formation of intra- and extradiol products in a 1:1 ratio suggests an equal probability of acyl and alkenyl migration rearrangements of the alkylperoxide intermediate. Bugg et al.[2] have proposed that the fate of the alkylperoxide intermediate is governed by stereoelectronic factors. Alkenyl migration gives rise to extradiol cleavage as a result of a pseudoaxial arrangement of the alkylperoxide intermediate. This has been supported by a recent crystal structure of the alkylperoxide intermediate of iron(II)-containing homoprotocatechuate 2,3-dioxygenase reported by Kovaleva et al.,[4] where the peroxide assumes a pseudoaxial orientation with respect to the substrate ring. On the other hand, a pseudoequatorial arrangement of the peroxide leads to an acyl migration to give intradiol cleavage. The structure of the model complex reported in this work indicates that both arrangements of the alkylperoxide intermediate are possible as a result of a vacant coordination site created by labile carboxylate oxygens (O1 and O2) in solution. This is also supported by the structural data of complex **1** with longer Fe−O(carboxylate) distances. It has been shown that the trimeric unit of complex **1** is in equilibrium with mono and dinuclear species in solution. The ESI-MS data of the solution immediately after reacting **1** with O_2 show only a peak at m/z 481.91 with isotope distribution patterns calculated for $[\{(L)Fe(DBC)\} + H]^+$ ion. The ion peak corresponding to the trinuclear unit could not be observed. This suggests that a mononuclear complex reacts with dioxygen. This also explains a 1:1 formation of extra- and intradiol products and supports its mimicry relevance of a mononuclear enzyme.

Conclusions

In conclusion, we have isolated and structurally characterized a novel iron(III)−catecholate model complex of a tridentate facial *N*,*N*,*O*-donor ligand derived from a natural

amino acid, L-proline. The binding mode of ligand mimics the 2-his-1-carboxylate facial triad motif observed in the superfamily of nonheme iron enzymes. The extradiol cleavage in acetonitrile without the formation of any autooxidation product is the first of this kind with a model iron−catecholate complex of a 2-*N*-1-carboxylate ligand. The iron−catecholate complex is a potential functional model of extradiol-cleaving catechol dioxygenases. A detailed study to model the other enzymes in the family of 2-his-1-carboxylate facial triad with this ligand is currently under investigation.

Acknowledgment. This work was supported by the Department of Science and Technology (DST), Government of India (Project SR/S1/IC-10/2006). S.P. and P.H. are thankful to the Council of Scientific and Industrial Research (CSIR), India for fellowship. Crystal structure determination was performed at the DST-funded National Single Crystal Diffractometer Facility at the Department of Inorganic Chemistry, IACS.

Supporting Information Available: Crystallographic data in CIF file format. This material is available free of charge via the Internet at http://pubs.acs.org.